

1
2
3
4
5
6
7
8
9
10
11
12
13
14
15
16
17
18
19
20
21
22
23
24
25
26
27
28
29
30
31
32
33
34
35
36
37

Title: Creating a neuroprosthesis for active tactile exploration of textures

Authors: Joseph E. O'Doherty^{1,2*}, Solaiman Shokur^{3,4*}, Leonel E. Medina^{1,5}, Mikhail A. Lebedev⁶⁻⁹, Miguel A. L. Nicolelis^{†1,4,6,7,10-13}

* JEO and SS have contributed equally to this work

Affiliations:

- 1 Department of Biomedical Engineering, Duke University, Durham, NC, 27708, USA
- 2 Present address: Neuralink Corp., San Francisco, CA, 94110, USA
- 3 STI IMT, École Polytechnique Fédérale de Lausanne, Lausanne, Switzerland
- 4 Present address: Neurorehabilitation Laboratory, Associação Alberto Santos Dumont para Apoio à Pesquisa (AASDAP), São Paulo, Brazil, 05440-000
- 5 Present address: Departamento de Ingeniería Informática, Universidad de Santiago de Chile, Santiago, Chile
- 6 Department of Neurobiology, Duke University Medical Center, Durham, NC, 27710, USA
- 7 Duke Center for Neuroengineering, Duke University, Durham, NC, 27710, USA
- 8 Center for Bioelectric Interfaces of the Institute for Cognitive Neuroscience of the National Research University Higher School of Economics, Moscow, Russia,
- 9 Department of Information and Internet Technologies of Digital Health Institute, I.M. Sechenov First Moscow State Medical University, Moscow, Russia,
- 10 Department of Neurology, Duke University, Durham, NC, 27710, USA
- 11 Department of Neurosurgery, Duke University, Durham, NC, 27710, USA
- 12 Department of Psychology and Neuroscience, Duke University, Durham, NC, 27708, USA
- 13 Edmond and Lily Safra International Institute of Neuroscience, Macaíba, Brazil

† Corresponding author:

Miguel A. Nicolelis
210 Research Drive
Box 103905 Dept of Neurobiology
Duke University
Durham, NC 27710
nicoleli@neuro.duke.edu

38 **Abstract**

39

40 Intracortical microstimulation (ICMS) of the primary somatosensory cortex (S1) can
41 produce percepts that mimic somatic sensation and thus has potential as an approach to
42 sensorize prosthetic limbs. However, it is not known whether ICMS could recreate active texture
43 exploration—the ability to infer information about object texture by using one’s fingertips to scan
44 a surface. Here we show that ICMS of S1 can convey information about the spatial frequencies
45 of invisible virtual gratings through a process of active tactile exploration. Two rhesus monkeys
46 scanned pairs of visually identical screen objects with the fingertip of a hand avatar, controlled
47 via a joystick and later via a brain-machine interface, to find the one with denser virtual gratings.
48 The gratings consisted of evenly spaced ridges that were signaled through ICMS pulses
49 generated when the avatar’s fingertip crossed each ridge. The monkeys learned to interpret
50 these ICMS patterns evoked by the interplay of their voluntary movements and the virtual
51 textures of each object. Discrimination accuracy across a range of grating densities followed
52 Weber’s law of just-noticeable differences (JND), a finding that matches normal cutaneous
53 sensation. Moreover, one monkey developed an active scanning strategy where avatar velocity
54 was integrated with the ICMS pulses to interpret the texture information. We propose that this
55 approach could equip upper-limb neuroprostheses with direct access to texture features
56 acquired during active exploration of natural objects.

57

58 Introduction

59 Sensory neuroprostheses offer the promise of restoring perceptual function to people
60 with impaired sensation ^{1,2}. In such devices, diminished sensory modalities (e.g., hearing ³,
61 vision ^{4,5}, or cutaneous touch ⁶⁻⁸) are reenacted through streams of artificial input to the nervous
62 system, typically using electrical stimulation of nerve fibers in the periphery or neurons in the
63 central nervous system. Restored cutaneous touch, in particular, would be of great benefit for
64 the users of upper-limb prostheses, who place a high priority on the ability to perform functions
65 without the necessity to constantly engage visual attention ⁹. This could be achieved through the
66 addition of artificial somatosensory channels to the prosthetic device ¹. Such an approach would
67 endow persons suffering from limb loss ¹⁰⁻¹², paralysis ^{1,13} or somatosensory deficits with the
68 ability to perform active tactile exploration of their physical environment and aid in dexterous
69 object manipulation ¹⁴⁻¹⁷.

70 Previously we demonstrated that motor and sensory functions could be simultaneously
71 enacted through a bidirectional neuroprosthetic system, called a brain-machine-brain interface
72 (BMBI)¹⁸. In that demonstration, the active exploration enabled by our BMBI-driven
73 neuroprosthesis used a limited and fixed set of ICMS temporal patterns to generate artificial
74 sensory inputs that mimicked the sense of flutter-vibration. However, it remained unclear
75 whether the same approach could generalize to allow the use of natural haptic exploratory
76 procedures, where a person identifies the texture of objects and materials by scanning them
77 with the fingertips.

78 Normal haptic exploration of objects involves several stereotypic procedures, such as
79 static contact for temperature sensation, holding for weight, enclosure for gross shape, pressure
80 for hardness, contour following for exact shape and lateral fingertip motion for texture ¹⁹. Here
81 we developed a neuroprosthetic paradigm for restoring the sensation of fingertip motion against
82 texture. We hypothesized that ICMS pulses generated by exploratory movements over virtual

83 gratings and delivered to primary somatosensory cortex (S1) would allow discrimination of
84 texture coarseness.

85 **Results**

86 *Active texture encoding*

87 Two rhesus monkeys (monkey M and monkey N) were chronically implanted with
88 multielectrode cortical arrays¹⁸ (Supplementary Fig. S1). These animals explored virtual objects
89 on a computer screen using a realistic upper-limb avatar (Supplementary Fig. S2), which they
90 operated manually with a joystick (Fig.1a) or using a BMI. On each trial, a pair of rectangles
91 appeared either on the left or on the right side of the screen. The rectangles were visually
92 identical, but each was associated with an invisible tactile grating whose properties were
93 signaled by charge-balanced ICMS pulses applied to S1 (a region exhibiting left forearm
94 receptive fields for monkey M and left lower-limb receptive fields for monkey N). Each grating
95 consisted of evenly spaced vertical ridges, which were invisible to the monkeys. The spatial
96 frequency of the ridges, f , ranged from 0.5 to 4.0 ridges/cm; an untextured object with no ridges
97 ($f = 0$ ridges/cm) was also presented on some trials.

98 The behavioral task required the monkeys to probe the rectangles with the avatar's
99 fingertip, determine which of the two had a higher f , and to hold the avatar over that object for
100 the required interval, 2 s in most cases (Fig. 1b). The artificial sensation was encoded by
101 delivering a charge-balanced ICMS pulse each time the avatar fingertip crossed a ridge in a
102 grating. Thus, the pulse-trains of ICMS delivered on any given trial provided an artificial signal
103 that depended on the interplay between the movements of the avatar and the f of the textures of
104 the explored objects (Supplementary Movie S1). Movements at a constant velocity across a
105 grating with a given f produced an ICMS pulse train with a constant temporal pulse rate (Fig.
106 2a). Movements at a faster velocity across the same grating produced a pulse train with a
107 correspondingly higher pulse rate (Fig. 2b). Irregular movements produced temporally varying
108 ICMS pulse trains (Fig. 2c). The objects' adjacent spacing on the screen encouraged the

109 monkeys to rapidly shift the avatar from one object to the other and determine which one had a
110 denser grating. The monkeys were permitted to explore the objects in any sequence and enter
111 each object multiple times, to accumulate evidence, before making the selection. Accordingly,
112 the monkeys could select an object on the first pass (Fig. 2d,e) or employ several explorations
113 of individual objects (Fig. 2f) before making a final selection. Prior to these experiments, these
114 monkeys participated in other studies^{18,20,21} and became proficient in using the joystick and the
115 hand avatar and making decisions using ICMS pulse trains. However, none of the previous
116 experiments employed the particular ICMS encoding rule or the texture scanning paradigm
117 presented in the current study.

118 *Active texture discrimination*

119 Both monkeys learned the task rapidly, reaching high-performance levels (71% of
120 correct trials for monkey N, and 73% for monkey M) after 10 daily sessions of training (Fig.
121 3a,b). The average performance was above chance even in the first training session (64% for
122 monkey N and 56% for monkey M). For monkey M, task difficulty was increased gradually, with
123 a large difference in f introduced early in training, $\Delta f \geq 2$ ridges/cm; $\Delta f < 2$ ridges/cm after 3
124 sessions and the full range from $f = 0$ to $f = 3.5$ ridges/cm and a minimum $\Delta f = 0.5$ by the end of
125 the training. The range for monkey N was $f = 0$ to $f = 3.5$ ridges/cm at the onset of the training
126 and $f = 0$ to $f = 4$ by the end. The minimum difference between textures, Δf , was maintained at
127 0.5 for all sessions. Figure 3 c,d shows the behavioral performance after learning (11 and 12
128 recording sessions for monkeys M and N, respectively). Both monkeys performed better on
129 individual trials when presented with larger Δf between the two objects than for smaller Δf , as
130 might be expected. However, we observed an additional scaling of discrimination difficulty that
131 depended on the absolute scale of the spatial frequencies of the objects being compared. More
132 specifically, the psychometric functions for both monkeys were steeper for larger values of $\sum f$,
133 that is, steeper for the larger sum for the two objects being compared (Fig. 4a,b).

134 We quantified this phenomenon by estimating the just noticeable difference (JND), for
135 each presented spatial frequency²². We calculated, for each spatial frequency, the probability of
136 choosing a second comparison frequency as a function of the unsigned delta between the
137 standard stimulus and the comparison stimulus (Fig. S3). We found that the JND increased
138 proportionally to f (Fig. 4c), consistent with the Weber–Fechner law²³ and Steven’s power law
139²⁴. The results for monkey M could be described by the linear function $JND(f) = 0.47f +$
140 1.06 ($R^2 = 0.63$); $JND(f) = 0.37f + 0.77$ for monkey N ($R^2 = 0.95$).

141 There are a number of strategies that the monkeys could have used to compare the
142 textures. One viable option would be to use a consistent velocity when exploring both objects so
143 that any variation in ICMS pulse rate between the objects would be due to differences in spatial
144 frequency alone. Further analysis revealed that this was not the case. Indeed, both monkeys
145 used a distribution of speeds to sample the gratings (Fig. 5a) and could perform successful
146 discriminations across the majority of their operating range (Fig. 5b)—only having difficulty when
147 moving at very high speeds. Moreover, for the vast majority of trials, the average speeds used
148 to scan the two objects differed, even within the same trial. Monkey M sampled the two objects
149 with the same speed (delta speed < 1 cm/s) on fewer than 3% of trials, a finding that was not
150 explained by the trial outcome (wrong trials: 2.41%, correct trials: 2.82%; Fig. S4). Monkey N
151 used the same scanning speed for each target on only 3.85% of the trials (3.95% of the wrong
152 trials, 3.81% of the correct trials).

153 This variability in arm movements was sufficiently large that, in some cases, the
154 ordinality of spatial frequency of the textures was different from the ordinality of the ICMS pulses
155 rates. An example of one of these apparently paradoxical trials is given in Figure 5c. For this
156 trial, frequency of the right target ($F_R = 3.5$ ridge/cm) was higher than the left ($F_L = 2.5$
157 ridges/cm), but the actual ICMS pulse rate delivered for the left target was higher than for the
158 right (left: 200.2 Hz versus right: 103.1 Hz). This occurred because a faster avatar speed was

159 used to explore the left target as compared to the right. Despite this, the monkey was able to
160 accurately choose the target with the higher spatial frequency in this example.

161 We found many of these apparently paradoxical trials (n=1231, 12% of all trials) for
162 monkey N. The majority of these cases corresponded to frequency pairs with high FR+FL (Fig.
163 S5). Monkey N's success rate was significantly above chance for these trials (56.1%, $P < 0.001$,
164 one-tailed binomial test; Fig. 5d). There were fewer of these trials for monkey M (n=329, 6% of
165 all trials). For these trials, monkey M's performance did not reach significance (52.03%, $P =$
166 0.25, one-tailed binomial test).

167 *Brain-machine-brain interface with active texture discrimination*

168 Finally, we validated our stimulation paradigm in a closed-loop brain-machine-brain
169 interface (BMBI) with monkey M. For this task, the monkey was allowed to move its arms, but
170 the joystick was disconnected; instead the avatar arm—and task performance—was controlled
171 via the decoding of 90 simultaneously recorded right-hemisphere M1 neurons (Fig. 6a). We
172 found that monkey M was able to control the avatar arm to explore the objects with minimal
173 movement of its physical hand as can be seen in the examples shown in Figure 6b. Moreover,
174 when the hand did move, it made smaller movements with lower velocities than the
175 simultaneous movements of the cursor during BMI trials (n=63 trials; Fig. 6c), but the monkey
176 could still control the cursor using cortical activity alone (Supplementary Movie S2). The monkey
177 retained the ability to accurately discriminate between the targets using the BMI; consistent with
178 the non-BMI task, the monkey was significantly above chance in discriminating targets with Low
179 $\sum f$ (76%, $P = 0.02$, one-sided binomial test), but did not reach significance for medium (65%, $P =$
180 0.09) or high $\sum f$ (40%, $P = 0.21$; Fig. 6d).

181

182 **Discussion**

183 We have demonstrated a novel encoding strategy for texture representation using ICMS
184 pulses in somatosensory cortex. Using this new approach, two animals were able to

185 discriminate texture coarseness during active tactile exploration. Importantly, for this task, small
186 variations of arm velocity changed the stimulation frequency; the interpretation of the texture,
187 therefore, may have employed a dynamic integration of ICMS stimulation information with arm
188 proprioception feedback or corollary discharge of motor and sensory cortical regions²⁵. The
189 apparently paradoxical trials provided evidence for these possibilities: access to the movement
190 command or proprioceptive feedback about the movement is necessary to disambiguate the
191 exafference of the texture from the reafference due to movement.

192 We observed that both monkeys were better at discriminating textures when the overall
193 spatial frequencies were small, consistent with the Weber-Fechner law²⁶, a phenomenon
194 reported for numerous sensory modalities²⁷, including touch²⁸. Interestingly, this law was
195 previously reported not to hold for the task of discriminating ICMS amplitude in primates²⁹ and
196 humans¹³. Our task, in contrast, required discriminating ICMS pulse rates, but, as it also used
197 active exploration we cannot rule out the possibility that some aspect of the effect is due to the
198 motor act itself.

199 Our tactile encoding scheme was effective for a single channel of independent tactile
200 information—mimicking a single mechanoreceptor localized in the fingertip. This encoding
201 scheme most closely resembles the rapidly adapting (RA) afferents of cutaneous somatic
202 sensation³⁰: each pulse of ICMS was triggered by the intersection of the active zone of the
203 avatar fingertip with a ridge on one of the gratings. However, there may be advantages of
204 modeling a more slowly adapting type-1 (SA1) encoding on some additional channels. We
205 believe that our encoding will be naturally extendable to arrays of mechanosensors embedded
206 in the “skin” of a prosthetic limb, with each sensor connected to a channel of microstimulation in
207 sensory cortex. For example, each feature in an object’s tactile microstructure could trigger a
208 pulse-train of ICMS that persists for some finite duration. This type of encoding may allow an
209 intuitive representation of the persistence of object-actuator contact interactions or complex
210 representation of natural textures³¹. However, a number of open questions remain, such as the

211 optimal timescale or distribution of timescales for adaptation and whether the degree of
212 adaptation must be matched to the properties of the specific neurons being stimulated. Work in
213 primates^{6,32} and rats³³ suggests that the plasticity of the brain will allow even a few channels of
214 stimulation to become effective at providing a rich sensory experience, and complex
215 spatiotemporal coding³⁴ with enough bandwidth to be clinically useful.

216 In our experiment, monkey N was superior to monkey M in perceiving small differences
217 of texture coarseness. While it is possible that this difference was due to a better
218 comprehension of the task by monkey N, it could also reflect the fact that the stimulation region
219 for monkey N was in the leg area while for monkey M it was in the receptive fields of the same
220 arm used to control the joystick. Therefore, it is possible that interference between feedback
221 from natural somatosensory pathways (hand touching the joystick, proprioception) and S1 ICMS
222 feedback made interpretation more difficult for monkey M. This indicates that further studies are
223 necessary to determine, among other things, the best target in S1 for delivering ICMS that
224 encodes tactile signals for future clinical neuroprosthesis. While delivering sensory feedback to
225 an ethologically meaningful cortical area is likely important for the subject to assimilate any limb
226 prosthesis as a natural appendage³⁵⁻³⁷, the use of different somatosensory regions in the
227 cortex may facilitate the sensory-motor integration and tactile acuity. Therefore, we suggest that
228 it may be necessary to deliver artificial sensory feedback to multiple cortical regions
229 simultaneously to achieve the best performance of such limb prostheses.

230 Recently demonstrated clinical neuroprostheses have used modulation of stimulation
231 amplitude (or equivalently, pulse-width) to encode the perception of pressure, force or position
232^{8,10,38,39}. Our approach is complementary—stimulation pulse timing encodes coarse texture—and
233 could be combined with the amplitude encoding approach to convey multimodal percepts of
234 pressure and texture. However some previous animal⁴⁰ and human⁴¹ stimulation studies have
235 provided indirect evidence that changes in pulse intensity (amplitude or pulse-width) may be
236 perceptually indistinguishable from changes in pulse rate. Further experiments will be necessary

237 to conclusively determine if this is the case or if there is in fact an extra degree of freedom that
238 can be used to convey clinically relevant prosthetic sensations.

239 Finally, we demonstrated that our encoding strategy could be integrated within a closed-
240 loop BMBI task. While the overall performance of the monkey for the BMBI task was lower than
241 during arm-control, the monkey was still able to discriminate the artificial textures. This, along
242 with the simplicity of our ICMS encoding, suggests that this approach could be used to equip
243 clinical upper-limb neuroprostheses with direct access to the tactile features of the natural world.

244

245 **Online methods**

246 All animal procedures were performed in accordance with the National Research
247 Council's Guide for the Care and Use of Laboratory Animals and were approved by the Duke
248 University Institutional Animal Care and Use Committee.

249 *Subjects and Implants*

250 Two adult rhesus macaque monkeys (*Macaca mulatta*) participated in the experiments
251 (monkeys M and N). Each monkey was implanted with four 96-microwire arrays constructed of
252 insulated stainless steel 304. Each hemisphere received two arrays: one in the upper-limb
253 representation area and one in the lower-limb representation area of sensorimotor cortex.
254 These arrays covered both M1 and S1; only microwires implanted in S1 were used for delivering
255 ICMS in study. For the BMI task, we used recordings from the right hemisphere arm arrays as
256 the monkey manipulated the joystick with the left arm. Within each array, microwires were
257 grouped in two four-by-fours, uniformly spaced grids each consisting of 16 electrode triplets.
258 The separation between electrode triplets was 1 mm. The electrodes in each triplet had three
259 different lengths, increasing in 300- μ m steps. The penetration depth of each triplet was
260 adjusted with a miniature screw. After adjustments during the month following the implantation
261 surgery, the depth of the triplets was fixed. The longest electrode in each triplet penetrated to a
262 depth of 2 mm as measured from the cortical surface.

263 *Task*

264 Each monkey sat in a primate chair, faced a computer screen and grasped a joystick
265 with their left hand. The joystick handle contained an optical sensor to indicate when the
266 monkey released it. The monkeys were trained to manipulate the joystick to control the
267 movements of a left upper-limb primate avatar on the screen^{18,42}.

268 Each trial began with a circular target appearing in the center of the screen. The
269 monkeys held an index finger of the avatar within this target for a random delay randomly drawn
270 from a uniform distribution parameterized from 200 to 2000 ms. After this delay, the central
271 target disappeared, and two rectangular object zones appeared on the screen. These appeared
272 either both on the left side or both on the right side of the screen at a distance of 7 cm from the
273 center. Both objects in the pair had the same width, (6 cm). The spacing between the objects
274 was 0.1 cm.

275 Vertical square-wave gratings were superimposed on each of the objects. These
276 gratings, which were not visible to the monkeys, were aligned on the center of each object and
277 were parameterized by spatial frequency, f . When the index finger of the avatar crossed a single
278 ridge in a grating, a pulse of ICMS was delivered to a pair of electrodes implanted in S1 cortex.
279 In this way, the pattern of ICMS delivered depended on the velocity of the avatar and the
280 intrinsic spatial frequency of each grating. The microstimulator was serviced at 100 Hz, which
281 meant that for sufficiently fast velocities or high spatial frequencies, it could be possible that
282 more than a single ridge was crossed in a 10 ms interval. If this occurred, we delivered N pulses
283 at $N*100$ Hz, where N was the number of ridges crossed since the last clock cycle. This
284 operation delivered the correct number of pulses at the correct rate, in expectation, at the cost
285 of up to 10 ms of latency.

286 Symmetric, biphasic, charge-balanced, cathode-leading ICMS pulses were delivered in a
287 bipolar fashion across pairs of microwires. The channels selected had clear sensory receptive
288 fields in the left forearm (monkey M: two pairs of microwires) or left lower limb (monkey N: one

289 pair of microwires). For monkey M, the cathodic and anodic phases of stimulation had a pulse
290 width of 105 μ s; for monkey N, the pulse phases were each 200 μ s. The cathodic and anodic of
291 the stimulation waveforms were separated by a 25 μ s interphase interval. The pulse amplitudes
292 were set to the minimal effective current, as found through psychometric measurements
293 separately for each monkey⁴³.

294 Monkeys received a reward for selecting the object from the pair with the higher spatial
295 frequency, f , drawn from:

$$296 \quad f \in \{0, 0.5, 1.0, 1.5, 2.0, 2.5, 3.0, 3.5, 4.0\} \text{ ridges/cm}$$

297 with the constraint that both objects did not share the same f on a single trial. Monkey M did not
298 discriminate the gratings as reliably and so was not presented any gratings with the highest
299 spatial frequency, 4.0 ridges/cm. The monkeys indicated their choice by holding the avatar over
300 one of the objects for the hold interval (2 seconds for the hand control and 1 second for the
301 BMBI task). Selecting the object with the higher f triggered the delivery of a fruit juice reward;
302 selecting the object with lower f ended the trial without reward.

303 The objects could be explored in any sequence. Moreover, objects could be re-explored
304 and re-compared multiple times in a trial. However, the avatar had to pass over both objects at
305 least once per trial. Trials for which only a single object was explored were terminated without
306 reward, even if the correct object was ultimately selected. Trials for which the monkey released
307 the joystick handle at any time, selected the wrong object, made a selection without exploring
308 both objects, or held the avatar outside of either of the objects for 10 s, resulted in the
309 termination of a trial and penalty interval of 2 s for monkey M and 2.5 s for monkey N.

310 We employed correction trials. This meant that after an incorrect trial, the next one
311 repeated with the same object locations and object-frequency identities. These correction trials
312 were used to keep the monkeys motivated and to prevent them from acquiring systematic

313 biases. As the rewarded object was known to the monkeys for correction trials, we excluded
314 these trials from all analyses.

315

316 *BMI decoding*

317 A 10th-order Unscented Kalman filter (UKF) was used for BMI predictions, using
318 methods we previously described^{18,44}. The filter parameters were fit using the hand movements
319 made while the task was performed using a joystick. The monkey was permitted to continue
320 moving the joystick, but was only rewarded for target selections made with the brain-controlled
321 cursor.

322

323 **References and Notes:**

- 324 1. Lebedev, M. A. & Nicolelis, M. A. L. Brain – machine interfaces: past , present and
325 future. **29**, (2006).
- 326 2. Collinger, J. L., Gaunt, R. A. & Schwartz, A. B. Progress towards restoring upper limb
327 movement and sensation through intracortical brain-computer interfaces. *Curr. Opin.*
328 *Biomed. Eng.* (2018). doi:10.1016/j.cobme.2018.11.005
- 329 3. Wilson, B. S. *et al.* Better speech recognition with cochlear implants. *Nature* **352**, 236–
330 238 (1991).
- 331 4. Humayun, M. S. *et al.* Visual perception in a blind subject with a chronic microelectronic
332 retinal prosthesis. *Vision Res.* **43**, 2573–2581 (2003).
- 333 5. Normann, R. A., Maynard, E. M., Rousche, P. J. & Warren, D. J. A neural interface for a
334 cortical vision prosthesis. *Vision Res.* **39**, 2577–2587 (1999).
- 335 6. Fitzsimmons, N. A., Drake, W. & Hanson, T. L. Primate reaching cued by multichannel
336 spatiotemporal cortical microstimulation. *J. Neurosci.* (2007). at
337 <<http://www.jneurosci.org/content/27/21/5593.short>>
- 338 7. Romo, R., Hernández, A., Zainos, A. & Salinas, E. Somatosensory discrimination
339 based on cortical microstimulation. *Nature* **392**, 387–390 (1998).
- 340 8. Tan, D. W. *et al.* A neural interface provides long-term stable natural touch perception.
341 *Sci. Transl. Med.* (2014). doi:10.1126/scitranslmed.3008669
- 342 9. Atkins, D. J., Heard, D. C. Y. & Donovan, W. H. Epidemiologic Overview of Individuals
343 with Upper-Limb Loss and Their Reported Research Priorities. *J. Prosthetics Orthot.* **8**, 2
344 (1996).
- 345 10. Raspopovic, S. *et al.* Supplementary materials for: Restoring natural sensory feedback in
346 real-time bidirectional hand prostheses. *Sci. Transl. Med.* **6**, 222ra19 (2014).
- 347 11. Marasco, P. D., Schultz, A. E. & Kuiken, T. A. Sensory capacity of reinnervated skin after
348 redirection of amputated upper limb nerves to the chest. *Brain* (2009). at

- 349 <<http://brain.oxfordjournals.org/content/132/6/1441.short>>
- 350 12. Oddo, C. M. *et al.* Intraneural stimulation elicits discrimination of textural features by
351 artificial fingertip in intact and amputee humans. *Elife* **5**, 1–27 (2016).
- 352 13. Flesher, S. N. *et al.* Intracortical microstimulation of human somatosensory cortex. *Sci.*
353 *Transl. Med.* **8**, 361ra141-361ra141 (2016).
- 354 14. Moberg, E. Criticism and study of methods for examining sensibility in the hand*.
355 *Neurology* (2012). doi:10.1212/wnl.12.1.8
- 356 15. Flanagan, J. R. & Wing, A. M. Modulation of grip force with load force during point-to-
357 point arm movements. *Exp. Brain Res.* **95**, 131–143 (1993).
- 358 16. Johansson, R. S. & Westling, G. Roles of glabrous skin receptors and sensorimotor
359 memory in automatic control of precision grip when lifting rougher or more slippery
360 objects. *Exp. Brain Res.* (1984). at
361 <<http://www.springerlink.com/index/M402455817334028.pdf>>
- 362 17. Johansson, R. S. & Flanagan, J. R. Coding and use of tactile signals from the fingertips in
363 object manipulation tasks. *Nat. Rev. Neurosci.* **10**, 345–359 (2009).
- 364 18. O'Doherty, J. E. *et al.* Active tactile exploration using a brain–machine–brain interface.
365 *Nature* **479**, 228–231 (2011).
- 366 19. Lederman, S. J. & Klatzky, R. L. Hand movements: A window into haptic object
367 recognition. *Cogn. Psychol.* (1987). doi:10.1016/0010-0285(87)90008-9
- 368 20. O'Doherty, J. E., Lebedev, M. A., Li, Z. & Nicolelis, M. A. L. Virtual active touch using
369 randomly patterned intracortical microstimulation. *IEEE Trans. Neural Syst. Rehabil. Eng.*
370 **20**, 85–93 (2012).
- 371 21. Medina, L. E., Lebedev, M. A., O'Doherty, J. E. & Nicolelis, M. A. L. Stochastic
372 Facilitation of Artificial Tactile Sensation in Primates. *J. Neurosci.* (2012).
373 doi:10.1523/jneurosci.3115-12.2012
- 374 22. Ulrich, R. & Vorberg, D. Estimating the difference limen in 2AFC tasks: Pitfalls and

- 375 improved estimators. *Attention, Perception, Psychophys.* (2009).
376 doi:10.3758/APP.71.6.1219
- 377 23. Gescheider, G. A. *Psychophysics: The fundamentals (3rd ed.)*. *Psychophysics: The*
378 *fundamentals (3rd ed.)*. (1997).
- 379 24. Stevens, S. S. On the psychophysical law. *Psychol. Rev.* (1957). doi:10.1037/h0046162
- 380 25. Crapse, T. B. & Sommer, M. A. Corollary discharge across the animal kingdom. *Nature*
381 *Reviews Neuroscience* (2008). doi:10.1038/nrn2457
- 382 26. Ekman, Gös. Weber's Law and Related Functions. *J. Psychol. Interdiscip. Appl.* (1959).
383 doi:10.1080/00223980.1959.9916336
- 384 27. Dehaene, S. The neural basis of the Weber-Fechner law: A logarithmic mental number
385 line. *Trends in Cognitive Sciences* (2003). doi:10.1016/S1364-6613(03)00055-X
- 386 28. Weber, E. H. *E.H. Weber on the Tactile Senses*. *E.H. Weber on the Tactile Senses*
387 (2018). doi:10.4324/9781315782089
- 388 29. Kim, S. *et al.* Behavioral assessment of sensitivity to intracortical microstimulation of
389 primate somatosensory cortex. *Proc. Natl. Acad. Sci.* **112**, 15202–15207 (2015).
- 390 30. Bolanowski, S. J., Gescheider, G. A., Verrillo, R. T. & Checkosky, C. M. Four channels
391 mediate the mechanical aspects of touch. *J. Acoust. Soc. Am.* (2005).
392 doi:10.1121/1.397184
- 393 31. Lieber, J. D. & Bensmaia, S. J. High-dimensional representation of texture in
394 somatosensory cortex of primates. *Proc. Natl. Acad. Sci.* (2019).
395 doi:10.1073/pnas.1818501116
- 396 32. Dadarlat, M. C., Doherty, J. E. O. & Sabes, P. N. A learning-based approach to artificial
397 sensory feedback leads to optimal integration. *Nat. Neurosci.* (2014).
398 doi:10.1038/nn.3883
- 399 33. Thomson, E. E., Carra, R. & Nicolelis, M. A. L. Perceiving invisible light through a
400 somatosensory cortical prosthesis. *Nat. Commun.* (2013). doi:10.1038/ncomms2497

- 401 34. Hartmann, K. *et al.* Embedding a Panoramic Representation of Infrared Light in the Adult
402 Rat Somatosensory Cortex through a Sensory Neuroprosthesis. *J. Neurosci.* **36**, 2406–
403 2424 (2016).
- 404 35. Rognini, G. *et al.* Multisensory bionic limb to achieve prosthesis embodiment and reduce
405 distorted phantom limb perceptions. *J. Neurol. Neurosurg. Psychiatry* (2018).
406 doi:10.1136/jnnp-2018-318570
- 407 36. Shokur, S. *et al.* Expanding the primate body schema in sensorimotor cortex by virtual
408 touches of an avatar. *Proc. Natl. Acad. Sci. U. S. A.* **110**, 15121–15126 (2013).
- 409 37. Collins, K. L. *et al.* Ownership of an artificial limb induced by electrical brain stimulation.
410 *Proc. Natl. Acad. Sci. U. S. A.* **114**, 166–171 (2017).
- 411 38. D'Anna, E. *et al.* A closed-loop hand prosthesis with simultaneous intraneural tactile and
412 position feedback. *bioRxiv* **8892**, 262741 (2018).
- 413 39. Graczyk, E. L. *et al.* The neural basis of perceived intensity in natural and artificial touch.
414 *Sci. Transl. Med.* **8**, 1–11 (2016).
- 415 40. Fridman, G. Y., Blair, H. T., Blaisdell, A. P. & Judy, J. W. Perceived intensity of
416 somatosensory cortical electrical stimulation. *Exp. Brain Res.* **203**, 499–515 (2010).
- 417 41. Fetz, E. E. *et al.* Direct electrical stimulation of the somatosensory cortex in humans
418 using electrocorticography electrodes: a qualitative and quantitative report. *J. Neural Eng.*
419 **10**, 036021 (2013).
- 420 42. Ifft, P. J., Shokur, S., Li, Z., Lebedev, M. A. & Nicolelis, M. A. L. A brain-machine interface
421 enables bimanual arm movements in monkeys. *Sci. Transl. Med.* **5**, (2013).
- 422 43. O’Doherty, J. E., Lebedev, M. A., Hanson, T. L., Fitzsimmons, N. A. & Nicolelis, M.
423 A. L. A Brain-Machine Interface Instructed by Direct Intracortical Microstimulation. *Front.*
424 *Integr. Neurosci.* **3**, (2009).
- 425 44. Li, Z. *et al.* Unscented Kalman filter for brain-machine interfaces. *PLoS One* (2009).
426 doi:10.1371/journal.pone.0006243

427 **Acknowledgments.** We thank D. Dimitrov for conducting the animal surgeries, J. Fruh for the
428 design of the monkey avatar, and G. Lehw, J. Meloy, T. Phillips, L. Oliveira, Amol Yadav and
429 S. Halkiotis for technical support. This research was supported by DARPA N66001-06-C-2019,
430 TATRC W81XWH-08-2-0119, and NIH Director's Pioneer Award DP1OD006798 to MALN.

431

432 **Author contributions.** JEO, MAL, and MALN designed the experiments. JEO, LEM, and MAL
433 conducted the experiments. JEO, SS, MAL, and MALN analyzed data and wrote the paper.

434

435 **Competing financial interests.** The authors declare no competing financial and/or non-
436 financial interests.

437

438 **Materials & Correspondence.** The custom code used for the experiments and the data that
439 support the findings of this study is available from the corresponding author upon reasonable
440 request. Requests should be addressed to nicoleli@neuro.duke.edu

441

442

443

444

445 **Figure Legends**

446

447 **Fig. 1. The artificial texture paradigm.** (a) A monkey is seated before a display on which an
448 avatar arm and two identical objects are projected. Artificial tactile feedback about the virtual
449 gratings associated with each object is delivered to populations of S1 neurons via temporal
450 patterns of ICMS as the monkey actively scans each object. (b) Trials commenced with a
451 random delay interval (1) when the monkey held the index finger of the avatar in the center of
452 the screen. Next, was the exploration interval (2). Two rectangular objects appeared, and the
453 monkey scanned these objects with the index finger of the avatar hand. Each object had an
454 associated virtual grating of vertical lines, which were invisible to the monkey. A pulse of ICMS
455 was delivered to a pair of electrodes in S1 with each crossing of the avatar index finger over a
456 line in one of the gratings. The trial was completed when the monkey indicated its selection (3)
457 by holding the avatar hand over one of the objects for a hold interval. The reward was delivered
458 if the monkey selected the object with the higher virtual grating frequency (inset); selecting the
459 object with the lower grating frequency ended the trial without reward.

460

461 **Fig. 2. The precise temporal pattern of ICMS delivered on any trial depended both on the**
462 **intrinsic spatial frequency of each object's virtual grating as well as the velocity with**
463 **which the monkey scanned each object.** For a grating with a given spatial frequency, slow
464 scanning (a) would produce a lower ICMS pulse rate than faster scanning (b). Irregular
465 scanning (c) of a grating produced irregular ICMS pulse trains. All other features of the pulse
466 train (e.g., current amplitude and pulse width) were fixed. (d-f). Examples of trials for three
467 values of Δf : (d) 3.5 (4.0 vs 0.5) ridges/cm, (e) 2.0 (2.0 vs 4.0) ridges/cm, and (f) 0.5 (2.0 vs 1.5)
468 ridges/cm, respectively. Traces indicate the x-component of the avatar position (solid lines) and
469 velocity (dashed lines). Gray rectangles indicate the position and horizontal dimension of the

470 objects. Red vertical lines indicate single pulses of ICMS. Trials started with a randomized hold-
471 time (200-2000 ms); a Go cue informed the monkey of the beginning of the exploration interval.

472

473 **Fig. 3. Monkeys discriminated spatial gratings based on self-generated temporal ICMS.**

474 **(a-d)** Percentage of trials for which the monkey chose the right-most object, parameterized by
475 the spatial frequencies of the right and left objects, for both monkeys. **(a,b)** The success rate at
476 the first session, and after three and after 10 sessions of training, is reported in parenthesis, and
477 the average percentage of trails for which the right object was chosen when $f_R > f_L$ and when
478 $f_L > f_R$, reported in yellow and blue, respectively. **(c,d)** The performance for all sessions (11
479 sessions for monkey N, $n=10412$ and 12 for monkey M, $n=5828$); monkey M was not presented
480 gratings with 4.0 ridges/cm. Asterisks indicate frequency-pair combinations which were
481 discriminated significantly differently than chance ($P < 0.05$, two-sided binomial test).

482

483 **Fig. 4. Psychometrics analysis of artificial texture discrimination. (a,b)** Discrimination of

484 spatial gratings obeys Weber's scaling for **(a)** monkey N and **(b)** monkey M. Each point
485 represents the percentage of trials for which the monkey chose the right-most object,
486 parameterized by the difference in spatial frequencies for a pair of objects (Δf , $f_R - f_L$) and the sum
487 of the spatial frequencies ($f_R + f_L$) for low (less than 2.5 ridges/cm, circles), mid (between 2.5 and
488 5 ridges/cm, diamonds) and high (greater than 5 ridges/cm, triangles) sums. Filled symbols
489 indicate discrimination significantly different than chance ($P < 0.05$, two-sided binomial test).

490 Error-bars indicate 95% confidence intervals. Curves are the sigmoid lines of best fit. **(c)** Just
491 noticeable differences (JNDs) for monkey M (diamonds) and N (circles), as a function of the
492 standard frequency (detail of JND calculation for each standard frequency is shown on Figure
493 S3; for monkey M JNDs for $f = 1$ and $f = 1.5$ were undefined). Linear fits, the corresponding
494 function and R^2 for each graph.

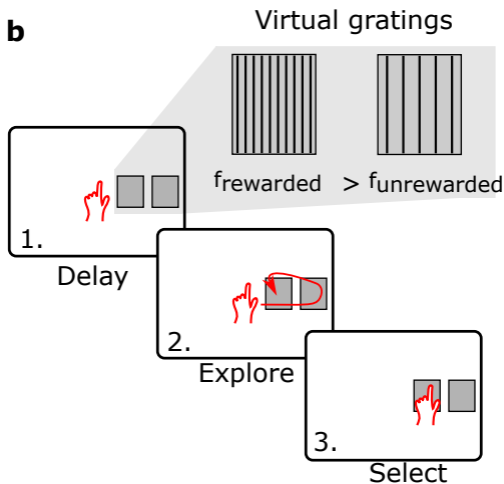
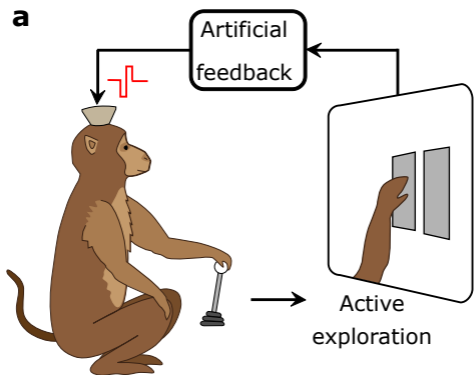
495

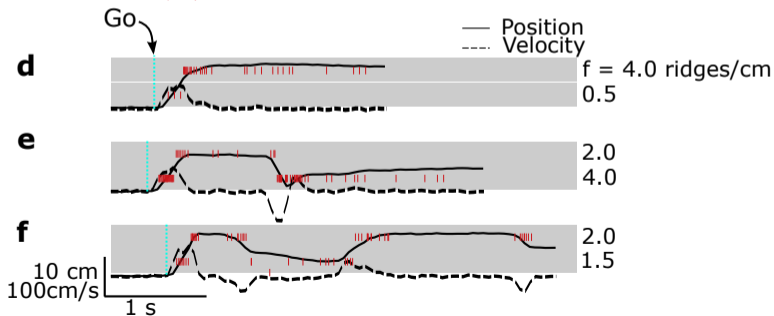
496 **Fig. 5. Texture perception and arm movement.** (a) Distribution of per-trial RMS exploration
497 speeds. (b) Percentage of trials performed correctly as a function per-trial RMS speed for
498 monkey M and monkey N. Curves are 4th order polynomial fits. Filled symbols indicate
499 discrimination significantly different than chance ($P < 0.05$, two-sided binomial test). (c) An
500 example of a paradoxical trial with monkey N. First two graphs indicate the x-component of the
501 avatar velocity and the x-position. Gray rectangles indicate the position and horizontal
502 dimension of the objects; their corresponding spatial frequencies were 2.5 and 3.5 ridges/cm,
503 respectively. Vertical red lines indicate single pulses of ICMS. ICMS pulse rate were calculated
504 for bursts of stimulation (a burst of stimulation was considered when the velocity magnitude was
505 maintained above 10 [cm/s]). (d) Success rate of the paradoxical trials. The chance level is
506 reported with a black dashed line. Error-bars indicate 95% confidence intervals (one-sided
507 binomial test).

508
509 **Fig. 6. BMI results** (a) Same experimental paradigm as in Fig 1a, expect that the control of the
510 avatar arm was done via decoding of motor intention from monkey's motor cortex. The monkey
511 has to hold the joystick during the task, was allowed to move the arm, but the joystick was
512 disconnected (b) Examples of two BMI trials and corresponding raster plots. Blue dashed lines
513 report the x projection of the brain-controlled cursor (BMI) and solid black line the monkey's
514 hand movement. ICMS pulses are shown with red vertical lines. Vertical dashed cyan line is the
515 end of the hold time (or onset of exploration), and solid green line is the end of the trial and
516 reward. Raster plots for the trials are grouped between 90 neurons in right hemisphere motor
517 cortex area (R-M1), 47 neurons in right hemisphere sensory area (R-S1) and five neurons in the
518 left hemisphere sensory area. (c) The distributions of velocity for the BMI controlled cursor
519 (blue) distribution of the monkey's hand movements (orange). The hand movement was
520 measured via the joystick movement (using the same gain as for hand control trials) and the trial
521 was aborted if the monkey released the joystick handle. (d) Percentage success for BMI

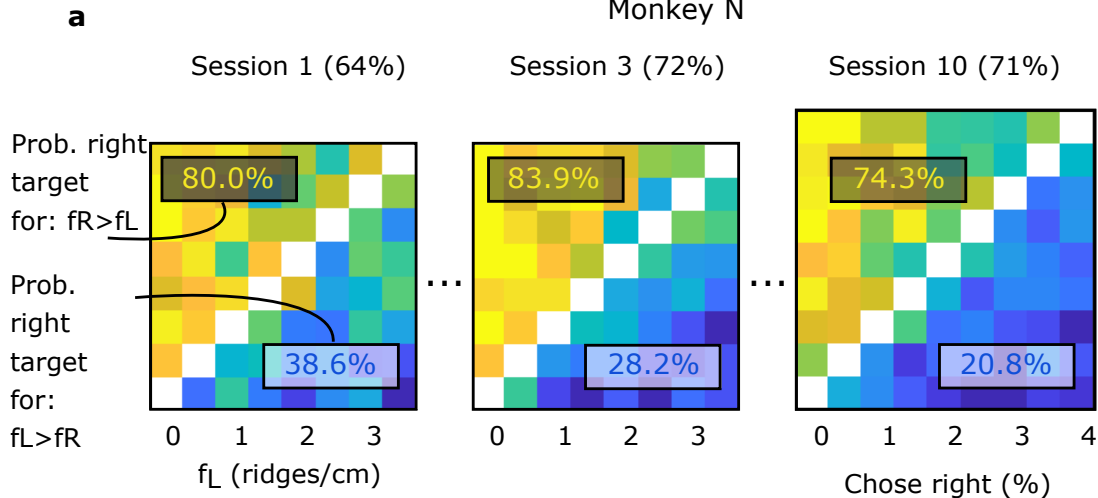
522 controlled trials, parameterized by the sum of the spatial frequencies (f_R+f_L) for low (less than
523 2.5 ridges/cm), mid (between 2.5 and 5 ridges/cm) and high (greater than 5 ridges/cm) sums.
524 Error-bars indicate 95% confidence intervals. Filled symbols are statistically different than
525 chance ($P<0.05$, one-sided binomial test).

526

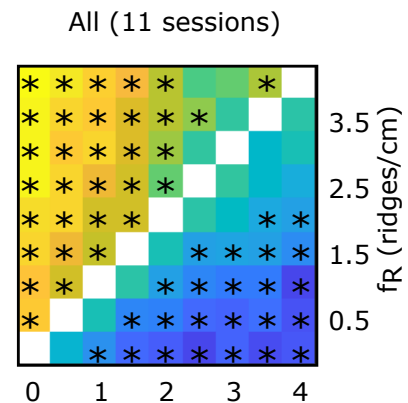




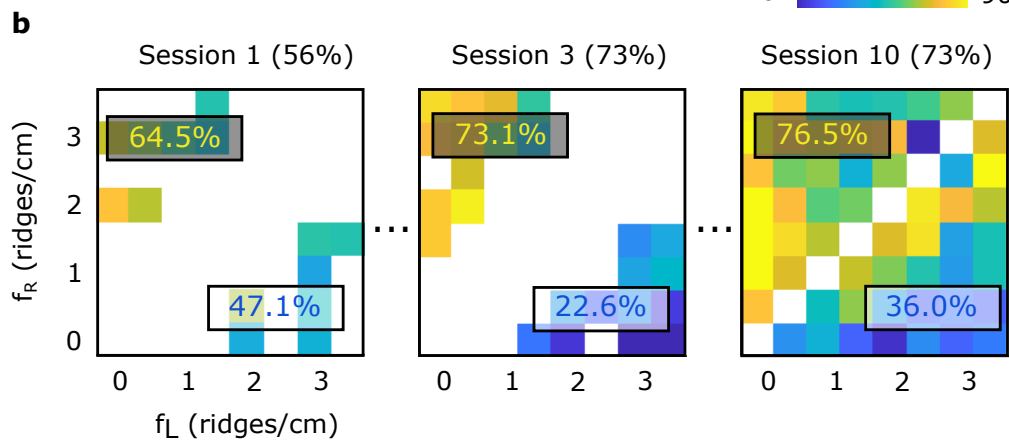
Monkey N



c



Monkey M



d

